

## $\alpha$ decay as a probe for phase transitions in nuclei

D. S. Delion,<sup>1</sup> A. Florescu,<sup>1</sup> M. Huyse,<sup>2</sup> J. Wauters,<sup>2,\*</sup> P. Van Duppen,<sup>3</sup>  
ISOLDE Collaboration,<sup>3</sup> A. Insolia,<sup>4</sup> and R. J. Liotta<sup>5</sup>

<sup>1</sup>*Institute of Atomic Physics, Bucharest Magurele, P.O. Box MG-6, Romania*

<sup>2</sup>*Leuven Isotope Separation On-Line (LISOL), Institute voor Kern-en Stralingsfysika KU Leuven,  
Celestijnenlaan 200 D, B-3001 Leuven, Belgium*

<sup>3</sup>*CERN, CH-1211 Geneva 23, Switzerland*

<sup>4</sup>*Department of Physics, University of Catania and INFN, I-95129 Catania, Italy*

<sup>5</sup>*Royal Institute of Technology at Frescati, S-10405 Stockholm, Sweden*

(Received 18 December 1995)

A microscopic description of alpha decay to intruder  $0_2^+$  states in the lead region is presented. The role played by proton-neutron correlations is emphasized. The calculated hindrance factors of transitions to the states  $0_2^+$  with respect to the corresponding ground state transitions are in good agreement with available experimental data. The abrupt variations in the measured hindrance factors in some cases are related to shape transitions. Predictions for further measurements are given. [S0556-2813(96)03509-1]

PACS number(s): 23.60.+e, 21.60.Jz, 27.80.+w

### I. INTRODUCTION

Recently there has been an increasing interest, both experimentally and theoretically, in studies of intruder  $0_2^+$  states near closed shell nuclei, particularly in the lead region. These states were experimentally observed first in two-neutron transfer reactions [1] and later in gamma spectroscopy [2,3], in alpha-decay experiments [4], and in inelastic reactions [5]. In a spherical core one expects the intruder  $0^+$  states to appear as a manifestation of two-phonon vibrations. There should be three  $0^+$  states of this type, namely, one induced by surface vibrations (in Gd [6] and in Pb [7] isotopes it is the octupole vibration) and two by pairing vibrations, corresponding to neutron and proton excitations. Yet, in the nucleus  $^{208}\text{Pb}$  only two of these three states were observed by inelastic scattering [5] and two-neutron transfer reaction [1] probes. It was found that this is due to a very small mixing of the proton pairing excitation, predicted at 5.5 MeV, with the other two two-phonon states [7]. For lighter lead isotopes the energies of the states  $0_2^+$  decrease with decreasing neutron number [8]. These states have recently been found to be largely populated by alpha decay probes in the isotopes  $^{190,192,194}\text{Pb}$  [9,10]. One puzzling feature in these measurements is that the hindrance factor of the alpha transition feeding the  $0_2^+$  relative to the ground state decreases as the excitation energy decreases, i.e., as one goes towards lighter lead isotopes. But perhaps the most striking feature of these experiments is that the hindrance factor changes abruptly, from 1.1 to about 80, when departing by a few protons from the  $Z=82$  closed shell [9,10]. This may be a sign of an unusual process occurring in these nuclei.

Several theoretical descriptions have been proposed for the intruder  $0^+$  states. In normal systems they were explained as a mixing of two-phonon surface and two-phonon

pairing excitations [7]. The monotone decrease of the excitation energy versus decreasing neutron number was proposed to be due to the quadrupole-quadrupole interaction between the proton and neutron systems. This study was done in the framework of a proton-neutron interacting boson model (IBM-2) [8] and within a quasiparticle phonon model [11]. The calculation of Ref. [8] suggests that the rather small deformations that are associated with the configurations that determine the  $0_2^+$  states are induced by the proton-neutron interaction, as is also suggested by calculations performed within a spherical shell-model basis in other nuclear systems [12–14]. Even the shape transition and coexistence of different shapes manifested in intruder proton states [15] may be partly due to proton-neutron correlations.

To analyze the fine structure observed in the alpha decay process  $\text{Po} \rightarrow \text{Pb}$  it is necessary to estimate the formation amplitude of the alpha clustering process on the nuclear surface [16–18].

The aim of the present paper is to give a microscopic description of the intruder  $0_2^+$  states in Pb isotopes and of the corresponding hindrance factors. For this we will describe the ground states within the random phase approximation (RPA) and the excited  $0_2^+$  states in terms of two-particle–two-hole (2p-2h) excitations on the RPA vacuum. For isotopes with proton number away from  $Z=82$  we will use a simpler model which, although phenomenological, contains ingredients that allow one to interpret the brusque change of the hindrance factor as a signature of a transition from spherical to deformed shapes. A short account of these calculations have been presented in Ref. [16].

The formalism is given in Sec. II, applications are in Sec. III, and a summary and conclusions are in Sec. IV.

### II. FORMALISM

We will study the alpha decay process

$$B \rightarrow A + \alpha \quad (2.1)$$

\*Present address: Department of Physics and Astronomy, University of Tennessee, Knoxville, Tennessee 37996.

within the two-step mechanism of Ref. [17]. First the four nucleons are clustered at some point on the nuclear surface and afterwards the already formed  $\alpha$  cluster penetrates the Coulomb barrier. This requires that one should be able to describe the formation of the alpha particle in the mother nucleus well beyond the nuclear surface, where the effects of the nucleons in the daughter nucleus are felt by the other nucleons only through the Coulomb interaction. In particular, in that region the Pauli principle acting among the nucleons in the two outgoing fragments is negligible. If this condition is fulfilled, the total width can be factorized in two parts

$$\Gamma(R) = P(R) \gamma^2(R), \quad (2.2)$$

where  $P(R)$  is the penetration factor through the Coulomb barrier at the distance  $R$  between the center of mass of the daughter  $A$  and the emitted alpha cluster, and

$$\gamma^2(R) = \frac{\hbar^2 R}{2M} |F(R)|^2 \quad (2.3)$$

is the so-called reduced decay width.  $F(R)$  is the formation amplitude of the alpha cluster at the radius  $R$ , i.e.,

$$F_L(R) = \int d\xi_\alpha d\xi_A d\Omega \{ \phi_\alpha(\xi_\alpha) \psi_A(\xi_A) Y_L(\Omega) \}_{J_B M_B}^* \psi_B(\xi_B), \quad (2.4)$$

where  $\psi_B$ ,  $\psi_A$ , and  $\phi_\alpha$  are the internal wave functions of the mother, daughter, and  $\alpha$ -particle nuclei, respectively

If the decay width is strongly dependent upon  $R$ , the theory would make no sense, since one may then choose an appropriate value of  $R$  to fit the experimental decay width. Actually this is a positive feature of the theory because it provides a self-consistent way of controlling that the conditions mentioned above are fulfilled. That is, the description of the  $\alpha$ -decay process would be trustworthy if the decay width, Eq. (2.2), would have a quasicontant behavior as a function of  $R$  in a region around the nuclear surface [18].

Usually the penetration factor in Eq. (2.2) depends very strongly on the excitation energy. In order to compare the ground-state to ground-state alpha decay process with the corresponding decay to an excited  $0^+$  state it is more convenient to introduce the hindrance factor (HF), which is just the ratio between the two corresponding formation amplitudes:

$$\text{HF} = \frac{|F(R; 0_1^+ \rightarrow 0_1^+)|^2}{|F(R; 0_1^+ \rightarrow 0_2^+)|^2}. \quad (2.5)$$

Light lead isotopes can be described within a spherical BCS representation consisting of neutron degrees of freedom [19]. But as one departs from  $^{208}\text{Pb}$  the proton core becomes softer and one needs to include explicitly the proton degrees of freedom also, especially for the so-called ‘‘intruder’’ state  $0_2^+$ .

While going from  $^{208}\text{Pb}$  towards lighter lead isotopes the spectra show the rare feature of states that are built upon spherical degrees of freedom coexisting with deformed states [10,15,19]. This process is even more conspicuous for nuclei with a few protons outside  $Z=82$ . We will therefore study these two regimes within two different models. The intruder states in lead will be described microscopically in terms of

pairing vibrations. In nuclei outside  $Z=82$  we will describe the states  $0^+$  within a simple two-dimensional basis consisting of the  $0_1^+$  and  $0_2^+$  states calculated before.

### A. Proton-neutron pairing vibration model

For light lead isotopes we will evaluate all wave functions microscopically within a spherical harmonic oscillator basis. Since our interest will be focused on  $0^+ \rightarrow 0^+$  transitions, one has in Eq. (2.4) that  $L = J_B = 0$  and the formation amplitude can be written in terms of a coherent superposition of harmonic oscillator wave functions  $\Phi_{N_\alpha L_\alpha=0}(R)$ . One can then perform the integrals analytically, since the internal wave function of the  $\alpha$  particle itself can be written as a product of  $0s$  states [20]. That is, expanding the mother and daughter wave functions  $\psi$  in terms of a harmonic oscillator basis and assuming a monopole coupling for the proton-proton and neutron-neutron interactions, one obtains [18]

$$F(R) = \sum_{N_\alpha} \Phi_{N_\alpha}(R) \sum_{j_k l} G_{N_\alpha}^\pi(j_k) G_{N_\alpha}^\nu(j_l) \times \langle B | (c_{\pi j_k}^\dagger c_{\pi j_k}^\dagger)_0 (c_{\nu j_l}^\dagger c_{\nu j_l}^\dagger)_0 | A \rangle, \quad (2.6)$$

where  $\tau j_k$  denotes the set of quantum numbers that label the single-particle spectra. For protons (neutrons) it is  $\tau = \pi(\nu)$ . The corresponding creation operators are denoted by  $c_{\tau j_k}^\dagger$ . The coefficients  $G_{N_\alpha}^\tau(j_k)$  contain recoupling geometrical factors and Moshinsky brackets that appear when transforming to center-of-mass and relative coordinates. Details of this can be found in Ref. [18]. In Eq. (2.6) the index  $L_\alpha$  was omitted in the harmonic oscillator wave function although  $L_\alpha=0$  is implied.

We have assumed in deriving Eq. (2.6) that the mother nucleus  $|B\rangle$  is in its ground state and the corresponding wave function is a product of proton and neutron BCS wave functions. The daughter nucleus  $|A\rangle$ , instead, will be left after the emission of the  $\alpha$  particle either in the ground state or in the excited  $0_2^+$  state. We will first assume that the state  $0_2^+$  is a two-particle–two-hole proton excitation on the ground state [15]. A simple description of such states can be given as the tensorial product of the particle times the hole pairing vibrations [7]. Since this is an important point which is basic for our model, we will present with some detail the proton-proton pairing modes and their use to construct the states  $0_2^+$ . But we want to stress that this is only for clarity of presentation, since light lead isotopes cannot be described within a spherical representation excluding proton-neutron interactions [19].

The RPA phonons describing the creation  $\Gamma_{\pi k}^\dagger(2)$  and annihilation  $\Gamma_{\pi k'}^\dagger(-2)$  of two protons are defined by the following relation:

$$\begin{pmatrix} \Gamma_{\pi k}^\dagger(2) \\ \Gamma_{\pi k'}^\dagger(-2) \end{pmatrix} = \begin{pmatrix} X_{\pi j_m}^k & Y_{\pi j_i}^k \\ Y_{\pi j_m}^{k'} & X_{\pi j_i}^{k'} \end{pmatrix} \begin{pmatrix} B_{\pi j_m}^\dagger \\ B_{\pi j_i}^\dagger \end{pmatrix}, \quad (2.7)$$

where

$$B_{\pi j_m}^\dagger = (c_{\pi j_m}^\dagger c_{\pi j_m}^\dagger)_0 \equiv \frac{1}{j_m} P_{\pi j_m}^\dagger B_{\pi j_i} = (c_{\pi j_i}^\dagger c_{\pi j_i}^\dagger)_0 \equiv \frac{1}{j_i} P_{\pi j_i}^\dagger \quad (2.8)$$

are the monopole proton operators entering the proton part of the formation amplitude (2.6). Here we denote states above the Fermi sea (particle states) by  $j_m, j_n$  and those below the Fermi sea (hole states) by  $j_i, j_j$ . When they are not specified we will use  $j_k, j_l$ . Notice that in Eq. (2.7) the operator  $\Gamma_{\pi k'}(-2)$  [and not  $\Gamma_{\pi k}^\dagger(-2)$ ] appears. One expects that the forward-going amplitudes  $X$  are, in absolute value, much larger than the backward-going amplitudes  $Y$  (the terms ‘‘forward going’’ and ‘‘backward going’’ are related to the ladder diagrams that correspond to the RPA in the two-particle Green function [21]). The RPA values of these amplitudes as well as the corresponding energies can be obtained from the equation of motion

$$[H, \Gamma_k^\dagger(\pm 2)] = E_k(\pm 2) \Gamma_k^\dagger(\pm 2). \quad (2.9)$$

For the monopole proton excitations that we want to describe the Hamiltonian is

$$H_\pi = \sum_{j_k} (\epsilon_{\pi j_k} - \lambda_\pi) N_{\pi j_k} - \frac{G_\pi}{4} \sum_{j_k j_{k'}} P_{\pi j_k}^\dagger P_{\pi j_{k'}}, \quad (2.10)$$

where  $N_{\pi j_k}$  is the particle number operator,  $P_{\pi j_k}^\dagger$  the pairing operator defined in Eq. (2.8),  $\epsilon_{\pi j_k}$  the single-particle energies for protons, and  $\lambda_\pi$  the Lagrange multiplier that is determined by the conservation, on average, of the total number of protons.

Defining the states  $0_2^+$  as a correlated two-particle–two-hole (2p-2h) excitation on the corresponding ground states, i.e., on the RPA vacua, one obtains

$$|0_2^+\rangle = \Gamma_{\pi k_1}^\dagger(2) \Gamma_{\pi k_2}^\dagger(-2) | \text{RPA} \rangle, \quad (2.11)$$

where  $k_1$  and  $k_2$  denote the first collective particle-particle and hole-hole RPA states, respectively. That is,  $k_1$  ( $k_2$ ) labels the particle (hole) pairing vibration. These collective states have the property that the wave function components  $X$  have all the same sign while the components  $Y$  have all the opposite sign. This property, which induces the enhancement of two-particle transfer form factors, can easily be understood within a separable interaction, as the pairing interaction that we are using, since the wave function components behave in this case as  $X_{\pi j_m}^k \sim 1/(2\epsilon_{\pi j_k} - E_k)$  and  $Y_{\pi j_m}^k \sim 1/(2\epsilon_{\pi j_k} + E_k)$  (notice that for the collective state it is  $|E_k| |2\epsilon_{\pi j_k}|$ ). These expressions also show that  $|X| > |Y|$ . These and other details on pairing excitations can be found in, e.g., Ref. [22].

In the harmonic approximation the energy of the state, Eq. (2.11), is given by

$$E_{0_2^+} = E_{k_2}(2) - E_{k_1}(-2). \quad (2.12)$$

These energies can be evaluated as a function of the strength parameter  $G_\pi$  in the pairing Hamiltonian (2.10). We have found that there are always reasonable values of  $G_\pi$  that

provide energies agreeing with experiment. However, the hindrance factors (HF's) calculated within this approach differ greatly with the corresponding experimental values. This failure is due to the fact that the proton-neutron interaction was neglected. That is, without the proton-neutron interaction the formation amplitude is just a product of proton and neutron parts, as will be shown below. As a result the neutrons participate in the 2p-2h excitation process only through the RPA vacuum, which is common for all the calculated  $0^+$  states, and in the ratio determining the hindrance factor (2.5) only the protons contribute, which is an unreasonable feature.

The simplest way to include the proton-neutron interaction is by generalizing the standard monopole pairing vibration. This has to be done consistently with the monopole character of the proton and neutron combinations entering the overlap in the formation amplitude (2.6). With this in mind, we define the two-particle creation operators as

$$\begin{pmatrix} \Gamma_k^\dagger(2) \\ \Gamma_{k'}(-2) \end{pmatrix} = \begin{pmatrix} X_{\tau j_m}^k & Y_{\tau j_i}^k \\ Y_{\tau j_m}^{k'} & X_{\tau j_i}^{k'} \end{pmatrix} \begin{pmatrix} B_{\tau j_m}^\dagger \\ B_{\tau j_i} \end{pmatrix}, \quad (2.13)$$

where now a summation over the index  $\tau = \pi, \nu$  is understood. The corresponding generalized pairing Hamiltonian is

$$\begin{aligned} H_{\pi\nu} = & \sum_{j_k} (\epsilon_{\pi j_k} - \lambda_\pi) N_{\pi j_k} + \sum_{j_k} (\epsilon_{\nu j_l} - \lambda_\nu) N_{\nu j_l} \\ & - \frac{G_\pi}{4} \sum_{j_k j_{k'}} P_{\pi j_k}^\dagger P_{\pi j_{k'}} - \frac{G_\nu}{4} \sum_{j_l j_{l'}} P_{\nu j_l}^\dagger P_{\nu j_{l'}} \\ & - \frac{G_{\pi\nu}}{4} \sum_{j_k j_l} (P_{\pi j_k}^\dagger P_{\nu j_l} + P_{\nu j_l}^\dagger P_{\pi j_k}), \end{aligned} \quad (2.14)$$

where the notation is as in Eq. (2.10). The formally simple proton-neutron Hamiltonian in Eq. (2.14), which we expect to account even for the slightly deformed configurations that determine the states  $0_2^+$ , violates isospin. But this violation may be small, since the mean value of the commutator  $[H, T_z]$  within BCS states vanishes. Notice that even  $[H, N\nu + N\pi]$ , where  $N\nu$  ( $N\pi$ ) is the neutron (proton) number operator, vanishes. Moreover, it is important in this context to mention that in the calculations below the strength  $G_{\pi\nu}$  is an order of magnitude smaller than the proton-proton and neutron-neutron strengths.

As before, the forward- and backward-going amplitudes can be obtained either by performing the commutators in the equation of motion (2.9) keeping only linear terms or by calculating the two-particle Green function within the ladder approximation. Both procedures provide the same RPA solutions.

Outside closed shell nuclei (e.g., light lead isotopes) the neutron system becomes superfluid and one can use a BCS representation. The formalism remains the same, but now the interaction matrix elements will depend on the occupation numbers  $U$  and  $V$  and the RPA equation becomes the quasi-random phase approximation (QRPA). Details of this can be found in, e.g., Ref. [19]. In our case the protons occupy normal orbits; that is, the numbers  $U$  and  $V$  have sharp dis-

tributions, and the proton system decouples into normal particle-particle, hole-hole, and particle-hole components, as in Ref. [7].

The state  $0_2^+$  is now

$$|0_2^+\rangle = \Gamma_{k_1}^\dagger (2) \Gamma_{k_2}^\dagger (-2) |\text{RPA}\rangle, \quad (2.15)$$

where the RPA vacuum has the structure [21]

$$|\text{RPA}\rangle = N \exp \left[ \sum_{\tau j_m j_i} Z_{j_m j_i}^\tau B_{\tau j_m}^\dagger B_{\tau j_i}^\dagger \right], \quad (2.16)$$

with  $N$  a normalization constant and

$$Z_{j_m j_i}^\tau = \sum_k Y_{\tau j_i}^k (X_{\tau j_m}^k)^{-1}. \quad (2.17)$$

The overlap entering the formation amplitude (2.6) corresponding to the  $0_1^+ \rightarrow 0_1^+$  decay becomes, to first order in  $XY$ ,

$$\langle B | (c_{\pi j_m}^\dagger c_{\pi j_m}^\dagger)_0 (c_{\nu j_n}^\dagger c_{\nu j_n}^\dagger)_0 | A \rangle = N U_{\pi j_m}^A V_{\pi j_m}^B U_{\nu j_n}^A V_{\nu j_n}^B \left( 1 - 2 \sum_{j_i} Z_{j_m j_i}^\pi - 2 \sum_{j_j} Z_{j_n j_j}^\nu \right), \quad (2.18)$$

while for the decay  $0_1^+ \rightarrow 0_2^+$  it is

$$\begin{aligned} \langle B | (c_{\pi j_m}^\dagger c_{\pi j_m}^\dagger)_0 (c_{\nu j_n}^\dagger c_{\nu j_n}^\dagger)_0 \Gamma_{k_1}^\dagger (-2) \Gamma_{k_2}^\dagger (2) | A \rangle = & 2N U_{\pi j_m}^A V_{\pi j_m}^B U_{\nu j_n}^A V_{\nu j_n}^B \left[ \sum_{j_{m'}} X_{\pi j_{m'}}^{k_1} X_{\pi j_{m'}}^{k_2} + \sum_{j_{i'}} Y_{\pi j_{i'}}^{k_1} X_{\pi j_{m'}}^{k_2} \right. \\ & - 2 \sum_{j_{m'} j_{i'}} X_{\pi j_{m'}}^{k_1} Y_{\pi j_{i'}}^{k_2} Z_{j_{m'} j_{i'}}^\pi + \sum_{j_{n'}} X_{\nu j_{n'}}^{k_1} X_{\nu j_{n'}}^{k_2} + \sum_{j_{j'}} Y_{\nu j_{j'}}^{k_1} X_{\nu j_{n'}}^{k_2} \\ & \left. - 2 \sum_{j_{n'} j_{j'}} X_{\nu j_{n'}}^{k_1} Y_{\nu j_{j'}}^{k_2} Z_{j_{n'} j_{j'}}^\nu \right]. \quad (2.19) \end{aligned}$$

The product  $UV$  in Eq. (2.18) is the usual one entering the ground-state to ground-state alpha decay formation amplitude [18]. The normalization  $N$  is common to all transitions and will thus cancel out in the evaluation of the hindrance factor.

One sees that without the proton-neutron interaction the hindrance factor only depends upon proton degrees of freedom, since in this case it is  $X_\nu = Y_\nu = 0$ .

## B. Two-level model

The detailed microscopic theory presented above cannot be applied when there are valence protons, besides the 2p-2h excitations, without including explicitly the additional degrees of freedom introduced by the valence protons, which eventually may even induce deformations in the assumed spherical core. It would be possible to construct such a theory, but it would be so complicated, both from a conceptual and a computational point of view, that it is questionable whether it is of any value to proceed along that line. But we can try to apply the experience gained above to describe the  $0^+$  states in those nuclei. That is, we have seen that the monopole-correlated states play a fundamental role in building up the intruder states. We have constructed the collective monopole vibrations starting from single-particle degrees of freedom. These vibrations were the building blocks that allowed us to calculate the  $0^+$  states in light lead isotopes. Now we can extend this procedure and use the most correlated of these  $0^+$  states as building blocks to describe the ground and intruder states of the other isotopes. This two-

level model to describe interacting bands was first proposed in Ref. [23], but was used in the spirit of this paper in Refs. [24,25].

The idea of calculating nuclear spectra in different steps, such that in each step one uses the correlated states calculated previously as building blocks, is behind the quasiparticle multistep shell-model method [19]. In a similar fashion we will use here as basis vectors the states  $0^+$  in the nuclei that are closest to the spherical core. That is, we choose  $^{194}\text{Pb}(\text{g.s.})$  and  $^{194}\text{Pb}(0_2^+)$  as basis vectors to describe neutron excitations,  $^{198}\text{Po}(\text{g.s.})$  and  $^{198}\text{Po}(0_2^+)$  as basis vectors to describe proton-particle excitations, and  $^{184}\text{Hg}(\text{g.s.})$  and  $^{184}\text{Hg}(0_2^+)$  for proton-hole excitations.

As in Refs. [9,16], we will call the basis vectors used to describe the mother nuclei by the letters  $u$  and  $v$ , e.g.,  $|u\rangle = |^{198}\text{Po}(\text{g.s.})\rangle$  and  $|v\rangle = |^{198}\text{Po}(0_2^+)\rangle$ , while the corresponding basis vectors for the daughter nuclei are  $|x\rangle = |^{194}\text{Pb}(\text{g.s.})\rangle$  and  $|y\rangle = |^{194}\text{Pb}(0_2^+)\rangle$ . These basis vectors are not the same as those use in Refs. [9,16].

Therefore the states in the mother nucleus will have the form

$$|0_1^+\rangle_m = a|u\rangle + b|v\rangle,$$

$$|0_2^+\rangle_m = -b|u\rangle + a|v\rangle. \quad (2.20)$$

The wave function amplitudes  $a$  and  $b$  are related by  $a^2 + b^2 = 1$ . In the daughter nucleus it is

$$\begin{aligned} |0_1^+\rangle_d &= c|x\rangle + d|y\rangle, \\ |0_2^+\rangle_d &= -d|x\rangle + c|y\rangle, \end{aligned} \quad (2.21)$$

with  $c^2 + d^2 = 1$ .

The hindrance factor can then be written as

$$\text{HF} = \left( \frac{d\langle 0_1^+ | T | 0_1^+ \rangle_m}{d\langle 0_2^+ | T | 0_1^+ \rangle_m} \right)^2 = \left( \frac{acT_1 + adT_2 + bcT_3 + bdT_4}{-adT_1 + acT_2 - bdT_3 + bcT_4} \right)^2, \quad (2.22)$$

where  $T_{i=1-4}$  is the matrix element of the operator  $T$  between the basis states, e.g.,  $T_1 = \langle x | T | u \rangle$ .

The expansion coefficients in Eqs. (2.20) and (2.21) are, in general, complex. Ideally, they are obtained after diagonalizing the many-body Hamiltonian. Taking these coefficients as real numbers, as we do here, their signs will not influence the unitarity of the transformations (2.20) and (2.21), although the value of Eq. (2.22) will change. A similar problem was found in Ref. [23]. In the applications below we determine these signs by fitting the HF for a given decay and keep the same sign for the other decays.

### III. APPLICATIONS

We will here apply the formalism described above. First the decay to light lead isotopes will be treated by using the microscopic model of Sec. II A and then the two-level model of Sec. II B will be applied to analyze the decay to isotopes outside  $Z=82$ .

#### A. Light lead isotopes

The ground states of the mother nuclei, i.e., Po isotopes, as well as the  $0^+$  states in the daughter lead nuclei will be described microscopically within a realistic single-particle basis consisting of the eigenvectors of a Woods-Saxon potential with the so-called universal parametrization [26]. The diagonalization of this potential will be performed by expanding the eigenfunctions in terms of spherical harmonic oscillator wave functions with size parameter corresponding to that of the alpha particle. The advantage of this choice is that the integrals in the formation amplitude (2.4) can all be performed analytically and the coefficients  $G$  in Eq. (2.6) can readily be evaluated [18]. To construct the RPA basis up to the shell  $N=5$  for protons and  $N=6$  for neutrons, up to two major shells above the Fermi level will be included.

The first step of the calculation is to evaluate the BCS parameters, particularly the occupation numbers  $U$  and  $V$  that enter in the QRPA matrix [19] as well as in Eqs. (2.18) and (2.19). For this we choose the pairing strength  $G_\nu = 0.1$  MeV, which provides values for the neutron pairing gaps that reproduce well the corresponding experimental values in  $^{190,192,194}\text{Pb}$  as well as in  $^{194,196,198}\text{Po}$ .

In the same fashion, we reproduce the proton gap in Po isotopes by taking  $G_\pi = 0.15$  MeV.

The strength  $G_{\pi\nu}$  can be evaluated by adjusting it to obtain the experimental energies of the intruder state according to the harmonic expression (2.12). This is an appealing prescription since the nonharmonic effects [neglected in Eq.

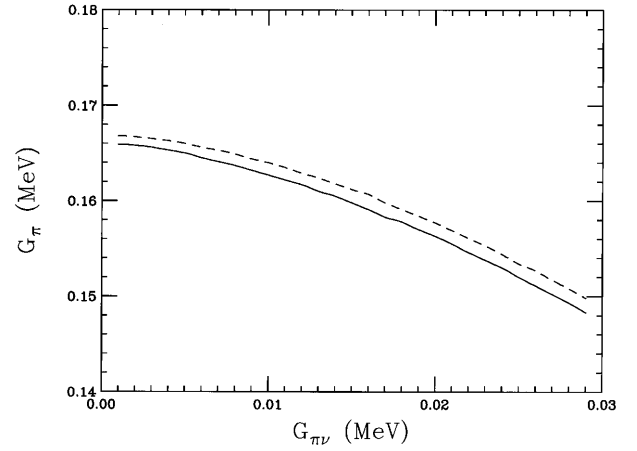


FIG. 1. Pairing strength  $G_\pi$  as a function of the strength  $G_{\pi\nu}$  for energies of the intruder state [Eq. (2.12)] of  $E_{0_2^+} = 1$  MeV (solid line) and 0.7 MeV (dashed line).

(2.12)] are due to the influence of the proton-neutron correlations. Choosing  $G_{\pi\nu}$  to simulate those effects seems to be a reasonable procedure of renormalizing the interaction. This is what one usually does with the strength  $\kappa_\lambda$  in effective interactions like separable or surface delta interaction (SDI) interactions, where  $\kappa_\lambda$  is adjusted to obtain the experimental energy of a state (usually the yrast) with angular momentum  $\lambda$  and parity  $(-1)^\lambda$  [21]. But in order to be acceptable, the value thus obtained for  $G_{\pi\nu}$  should be reasonable; i.e., it should be small in comparison to the strengths  $G_\pi$  and  $G_\nu$  (to minimize the effects of isospin violation) and it should not change drastically from nucleus to nucleus even as a function of the other strength parameters. To probe these points we show in Fig. 1 the relation between the strength parameters  $G_\pi$  and  $G_{\pi\nu}$  for a fixed energy of the intruder state. In this figure the cases  $E_{0_2^+} = 1$  MeV (solid line) and  $E_{0_2^+} = 0.7$  MeV (dashed line) are presented. The values of  $G_\pi$  are chosen in this figure in the neighborhood of the value that fits the proton gap ( $G_\pi = 0.15$  MeV). One sees that  $G_{\pi\nu}$  varies very smoothly and within a reasonable and rather small range in this figure. Moreover, a difference of 300 keV in the calculated energies (i.e., the difference between the two curves) requires very small changes in the parameters. That is, a rather wide range of reasonable values of the pairing strengths  $G_\pi$  and  $G_{\pi\nu}$  will all provide the energies of the intruder states. Perhaps even more important, the strength  $G_{\pi\nu}$  is about one order of magnitude smaller than the other strengths.

We thus choose the starting values of  $G_\pi$  and  $G_{\pi\nu}$  such that the HF corresponding to the state  $^{190}\text{Pb}(0_2^+)$  at the experimental energy is obtained. This is achieved with  $G_{\pi\nu} = 0.015$  MeV and  $G_\pi = 0.16$  MeV, which also fits reasonably well the experimental proton pairing gaps. This is expected since this value of  $G_\pi$  is very close to the one determined previously as ‘‘best choice’’ for that purpose (i.e.,  $G_\pi = 0.15$  MeV). From this point we varied  $G_{\pi\nu}$  (with the values of  $G_\nu = 0.1$  MeV and  $G_\pi = 0.16$  MeV fixed) to obtain the energies  $E_{0_2^+}$  as a function of  $G_{\pi\nu}$ . For each one of these points we calculated the BCS occupation parameters, the

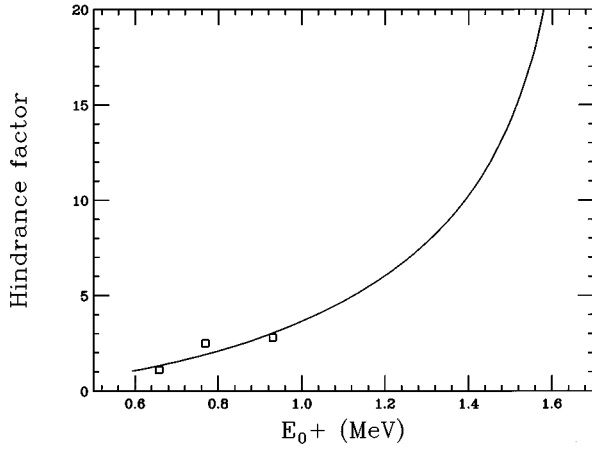


FIG. 2. Hindrance factor as a function of the energy of the intruder states  $0_2^+$  in Pb isotopes. The experimental data (squares) are taken from Ref. [10].

QRPA amplitudes  $X$  and  $Y$ , and the HF according to Eqs. (2.18) and (2.19). The results of the calculation are shown in Fig. 2. Notice that  $G_{\pi\nu}$  is chosen as a free parameter only at the starting point, i.e., the point of lowest energy in Fig. 2. Afterward we got the energies and the HF as a function of  $G_{\pi\nu}$  such that for a given energy of Fig. 2 one can assign the corresponding HF. For the measured energies of  $^{192,194}\text{Pb}$ , Fig. 2 shows that the calculated values of the HF agree very well with the corresponding experimental values. Moreover, we give in Fig. 2 also the values of the HF for higher energies in the hope that they may be useful as a guide in eventual experimental searches. In particular, we predict that going towards heavier lead isotopes, where the increasing energy of the intruder state would eventually lie above 5 MeV (in  $^{208}\text{Pb}$ ) [7], the HF increases very rapidly. Besides the problem that one may reach the decay threshold, Fig. 2 shows that even from a spectroscopy point of view an experimental detection of the intruder states in heavy lead isotopes through alpha-decay experiments would be difficult.

It is worthwhile also to notice from Figs. 1 and 2 that the increase in energy implies a decrease in the proton-neutron strength  $G_{\pi\nu}$  (with all other parameters fixed). Therefore when approaching the normal nucleus  $^{208}\text{Pb}$  the monopole proton-neutron correlation diminishes, as it should be since the superfluidity of the neutrons tends to disappear in this situation. Eventually, in the normal system, the different correlations are related to the decoupled particle-particle, hole-hole, and particle-hole states, as discussed in Ref. [7].

### B. Isotopes outside $Z=82$

Hindrance factors corresponding to decays to intruder states in the nuclei  $^{196,198}\text{Po}$ ,  $^{182,184}\text{Hg}$ , and  $^{176,178,180}\text{Pt}$  were recently measured [9,10]. The unexpected feature in this case is that the hindrance factors show large and sudden changes in some nuclei, as shown in Table I. In fact the HF corresponding to the decay of  $^{200}\text{Rn}$  is the largest,  $\Delta I=0$ , ever measured. As comparison one also sees in Table I the HF corresponding to the decay of the Po isotopes discussed above. There is a factor 80 between the HF measured in the

TABLE I. Calculated hindrance factor (HF) in proton-particle nuclei. The numbers  $a$  and  $c$  are the ground-state wave function amplitudes as defined in Eqs. (2.20) and (2.21), respectively. The component  $b(d)$  is given by the normalization condition.

Mother	Daughter	HF (HF <sub>expt</sub> )	$a$	$c$
$^{198}\text{Po}$	$^{194}\text{Pb}$	3.0 (2.8 $\pm$ 0.5)	1.00	1.00
$^{196}\text{Po}$	$^{192}\text{Pb}$	2.5 (2.5 $\pm$ 0.1)	0.99	0.99
$^{194}\text{Po}$	$^{190}\text{Pb}$	1.0 (1.1 $\pm$ 0.1)	0.82	0.98
$^{202}\text{Rn}$	$^{198}\text{Po}$	19 (19.0 $\pm$ 6)	-0.94	1.00
$^{200}\text{Rn}$	$^{196}\text{Po}$	78.8 (79 $\pm$ 7)	-0.95	0.99
$^{200}\text{Rn}$	$^{196}\text{Po}$	13295 (79 $\pm$ 7)	-0.92	0.99

decay of  $^{194}\text{Po}$  and the one in  $^{200}\text{Rn}$ . Furthermore, one notices a systematic trend in the HF values for the decay of Hg isotopes of Table II. In contrast to the decay of Pb isotopes, where the HF is essentially constant, the HF rises from 2.4 in  $^{184}\text{Hg}$  to 17 in the case of  $^{180}\text{Hg}$ . This outstanding feature may be the signature of an uncommon process occurring in nuclei.

In the cases of Table I, which we will analyze first, the active particles occupy particle states. As discussed in the previous section, we choose the basis vectors that will describe the states  $0^+$  as those corresponding to the decay of  $^{198}\text{Po}$ . Therefore for this decay it is  $a=1$ ,  $b=0$ ,  $c=1$ , and  $d=0$ .

The matrix elements  $T_i$  are in this case

$$T_1 = \langle ^{198}\text{Po}(\text{g.s.}) | T | ^{194}\text{Pb}(\text{g.s.}) \rangle,$$

$$T_2 = \langle ^{198}\text{Po}(\text{g.s.}) | T | ^{194}\text{Pb}(0_2^+) \rangle,$$

$$T_3 = \langle ^{198}\text{Po}(0_2^+) | T | ^{194}\text{Pb}(\text{g.s.}) \rangle,$$

and

$$T_4 = \langle ^{198}\text{Po}(0_2^+) | T | ^{194}\text{Pb}(0_2^+) \rangle,$$

where the operator  $T$  creates an  $\alpha$  particle. Since the basis states are just the modes that connect these transitions, it is  $|T_1| = |T_4|$ . In the matrix element  $T_2$  the operator  $T$  creates two protons in the two-proton hole states that are available in  $|^{194}\text{Pb}(0_2^+)\rangle$  while the neutrons occupy the superfluid states just leading to  $|^{198}\text{Po}(\text{g.s.})\rangle$ . A comparison of the experimental values for the alpha reduced widths [27] allows one to estimate that  $(T_1)^2$  is about 3 times  $(T_2)^2$ . Finally, in  $T_3$  the operator  $T$  can only create protons in states above the Fermi level, and since in the state  $|^{198}\text{Po}(0_2^+)\rangle$  there are unoccupied proton hole states, one gets  $T_3=0$ . One may argue that this

TABLE II. As in Table I for proton-hole nuclei.

Mother	Daughter	HF (HF <sub>expt</sub> )	$a$	$c$
$^{188}\text{Pb}$	$^{184}\text{Hg}$	21.1 (21 $\pm$ 3)	0.95	1.00
$^{186}\text{Pb}$	$^{182}\text{Hg}$	21.0 (21 $\pm$ 4)	0.92	0.90
$^{184}\text{Hg}$	$^{180}\text{Pt}$	0.62 (2.4 $\pm$ 0.4)	1.00	0.62
$^{182}\text{Hg}$	$^{178}\text{Pt}$	3.0 (3.5 $\pm$ 0.6)	0.90	0.71
$^{180}\text{Hg}$	$^{176}\text{Pt}$	130 (17 $\pm$ 5)	0.80	0.92

estimation of  $T_3$  is very crude because the real vacua are correlated states. However, it has to be considered that throughout this paper we are assuming that the shell  $Z=82$  is not badly broken as the number of neutrons decreases. This is an approximation that we accept, particularly in this section, to avoid introducing too many parameters, which would spoil the simplicity and elegance of the model. Besides, the main conclusions of this paper will not be changed if reasonable values of  $T_3$  are allowed [16].

The neutron-deficient Pb isotopes are quasispherical and have a rather sharply defined Fermi surface with a complete filled  $Z=82$  proton shell. This can be deduced from lifetime measurements of the  $\text{Pb}(0_2^+)$  states [28] as well as from the excitation energy of the states  $2_1^+$ . Therefore, within our model the mixing amplitude  $c$  is close to unity for all the Pb isotopes considered in Table I, starting with  $c=1$  in  $^{194}\text{Pb}$ , as mentioned above. This is in good agreement with the results of Ref. [28], from where we took the values of  $c$  for the other Pb isotopes in Table I.

For the mother Po isotopes in this table we start with  $a=1$  in  $^{198}\text{Po}$ , as also discussed above, obtaining  $\text{HF}=3$  for the corresponding alpha decay, in good agreement with experiment ( $\text{HF}=2.8\pm 0.5$ ). For the lighter Po isotopes we adjust the amplitude  $a$  to reproduce the experimental HF values. One notices in Table I that in  $^{194}\text{Po}$  the amplitude  $a$  is rather small, indicating that here mixing between the two  $0^+$  states appears.

The values of  $c$  in the decays of the Rn isotopes in Table I correspond to the wave functions of the now daughter Po isotopes. That is, the parameters  $c$  in this case are the parameters  $a$  in the decay of Po isotopes analyzed above, i.e.,  $c(^{198}\text{Po})=1.00$  and  $c(^{196}\text{Po})=0.99$ . The value of  $a$  in  $^{202}\text{Rn}$  was chosen such that it fits the corresponding HF value. One thus obtains that  $a$  is close to unity, but negative, as seen in Table I. This is an example of the determination of the signs of the wave function components in a given type of excitation (in this case proton particles) by adjusting the experimental data. From the nucleus  $^{202}\text{Rn}$  thus calculated, we analyzed next the decay of  $^{200}\text{Rn}$  by smoothly changing the corresponding wave function component  $a$ . But here we notice a very strong dependence of HF upon  $a$ . With  $a=-0.95$  we obtain the experimental HF, but with  $a=-0.92$  one obtains  $\text{HF}=13\,295$ , as shown in Table I. This is a typical feature of unstable systems that undergo a phase transition process. That is, the extremely large experimental HF value observed in the decay of  $^{200}\text{Rn}$  is a sign that a phase transition occurs in this nuclear region.

For the proton-hole excitations that appear in the decays of Pb and Hg isotopes the basis vectors are determined by the states  $^{184}\text{Hg}(\text{g.s.})$  and  $^{184}\text{Hg}(0_2^+)$ , as discussed above, with the assumption that the conditions  $T_1=T_4$ ,  $T_2=0$ , and  $(T_3)^2=3(T_1)^2$  are approximately fulfilled. That means that for the daughter nucleus  $^{184}\text{Hg}$  in Table II it is  $c=1$ . We determine the corresponding value of  $a$  by smoothly extrapolating the values of the neutron components in Table I (i.e., the values of  $c$  for  $^{194,192,190}\text{Pb}$ ). This would give  $a=0.97$ , very close to the value  $a=0.95$  which was chosen just to reproduce the experimental data for HF in Table II. Extrapolating one obtains  $a(^{186}\text{Pb})=0.92$  and with  $c(^{182}\text{Hg})=0.90$ ,

which is a rather smooth variation from the value  $c=1$  assigned to  $^{184}\text{Hg}$ , and one obtains again the experimental HF.

Finally, for the decay of Hg isotopes we take the wave functions previously evaluated, i.e.,  $a(^{184}\text{Hg})=1.00$  and  $a(^{182}\text{Hg})=0.90$ , and extrapolating for  $^{180}\text{Hg}$  one obtains  $a(^{180}\text{Hg})=0.80$ . The wave function components of the corresponding Pt isotopes are, according to Ref. [24],  $c(^{180}\text{Pt})=0.62$ ,  $c(^{178}\text{Pt})=0.71$ , and  $c(^{176}\text{Pt})=0.92$ . With these values of  $a$  and  $c$  one obtains values of the HF that are surprisingly close to the corresponding experimental values. Particularly the strong variation of the experimental HF going from  $^{182}\text{Hg}$  to  $^{180}\text{Hg}$  is strongly marked, indicating even here that a phase transition has taken place.

It is worthwhile to point out the simplicity of the model used in this section. This may be compared with the rather involved formalism used before.

#### IV. SUMMARY AND CONCLUSIONS

In this paper we have calculated hindrance factors (HF's) of alpha decay transitions into the ground state with respect to the corresponding intruder  $0_2^+$  transitions from Po, Rn, Pb, and Hg isotopes. The interest of this calculation lies in some puzzling features found in the corresponding experimental values that were recently reported [9,10]. In the decay to the intruder states of Pb isotopes the HF is small (and, therefore, the transitions to the intruder states are large) and decreases with decreasing energy of the intruder state. Already this is remarkable. But even more interesting is that for the other isotopes the HF may change drastically when going from one nucleus to its neighbor.

To understand these features we analyzed first light lead isotopes within the framework of a RPA calculation using standard pairing interactions for identical particles. We described the intruder states as a correlated two-particle-two-hole (2p-2h) proton excitation. As expected, we found that protons in the mother Po isotopes as well as in the intruder states in Pb move in normal orbits; i.e., the occupation numbers  $U$  and  $V$  have a sharp distribution in this case. We found that the energies of the intruder states calculated within this model can be fitted by appropriate choices of the proton pairing strength  $G_\pi$ . However, within this calculation we could not obtain the corresponding experimental energies and HF simultaneously. We ascribed this deficiency to the lack of a proper interaction between neutrons and protons, although the pairing strengths that are determined by fitting the experimental pairing gaps [21] partially include the proton-neutron ( $p$ - $n$ ) interaction in an effective way. To consider this interaction, we introduced a  $p$ - $n$  force that is a generalization of the standard pairing force but which violates isospin. We have argued that this violation is not large. We found that even in this case the protons mostly move in normal orbits but the 2p-2h excitations include now both neutrons and protons. We found that the dependence of the experimental HF upon the excitation energy of the intruder state (i.e., upon the  $p$ - $n$  strength  $G_{\pi\nu}$ ) is very well reproduced by the calculation. We obtained the experimental values in the three isotopes so far measured by choosing  $G_{\pi\nu}$  so as to reproduce the HF in one of those isotopes. We have even presented the calculated HF for other values of the en-

ergy in the hope that they may be useful as a guide in eventual experimental searches.

For the other cases observed experimentally we used a very simple model consisting of a basis that includes two states  $0^+$ , which represent the ground and intruder states without correlations [23,24]. By adjusting the mixing amplitude to reproduce the hindrance factor we observed that in  $^{194}\text{Po}$  a mixing between the ground state and the  $0_2^+$  state appears. In contrast, in Hg isotopes those mixings are small. We have also found that in light Pt isotopes a change in the

structure of the ground states occurs, confirming previous results [24]. Finally, we found that in the decay of Rn isotopes the HF is very sensitive to small changes in the corresponding wave functions. This is a typical feature of systems that undergo a phase transition. We therefore ascribed the large value of the HF observed in the decay of  $^{200}\text{Rn}$  to a phase transition in this nuclear region and, more generally, we conclude that the study of alpha decay hindrance factors may provide a powerful tool to detect those phase transitions.

- 
- [1] G. J. Igo, P. D. Barnes, and E. R. Flynn, *Phys. Rev. Lett.* **24**, 470 (1970).
- [2] Van Duppen, E. Coenen, K. Deneffe, M. Huyse, K. Heyde, and P. Van Isacker, *Phys. Rev. Lett.* **52**, 1974 (1984).
- [3] J. Kantele, M. Luontama, W. Trzaska, R. Julin, A. Passoja, and K. Heyde, *Phys. Lett. B* **171**, 151 (1986).
- [4] P. Van Duppen, E. Coenen, K. Deneffe, M. Huyse, and J. L. Wood, *Phys. Lett.* **154B**, 354 (1985).
- [5] R. Julin *et al.*, *Phys. Rev. C* **36**, 1129 (1987).
- [6] M. Piiparinen *et al.*, *Phys. Rev. Lett.* **70**, 150 (1993).
- [7] P. Curutchet *et al.*, *Phys. Lett. B* **208**, 331 (1988).
- [8] K. Heyde, J. Jolie, J. Moreau, J. Ryckebusch, M. Waroquier, P. Van Duppen, M. Huyse, and J. L. Wood, *Nucl. Phys.* **A466**, 189 (1987).
- [9] J. Wauters *et al.*, *Phys. Rev. Lett.* **72**, 1329 (1994).
- [10] J. Wauters *et al.*, *Phys. Rev. C* **50**, 2768 (1994).
- [11] V. G. Soloviev, *Z. Phys. A* **334**, 143 (1989); *Theory of Atomic Nuclei: Quasiparticles and Phonons* (Energoizdat, Moscow, 1989).
- [12] P. Federman and S. Pittel, *Phys. Rev. C* **20**, 820 (1979).
- [13] K. Heyde, P. Van Isacker, R. F. Casten, and J. L. Wood, *Phys. Lett.* **155B**, 303 (1985).
- [14] T. R. Werner, J. Dobaczewski, M. W. Guidry, W. Nazarewicz, and J. A. Sheikh, *Nucl. Phys.* **A578**, 1 (1994).
- [15] J. L. Wood, K. Heyde, W. Nazarewicz, M. Huyse, and P. Van Duppen, *Phys. Rep.* **215**, 101 (1992).
- [16] D. S. Delion, A. Florescu, M. Huyse, and J. Wauters, P. Van Duppen, the ISOLDE Collaboration, A. Insolia, and R. J. Liotta, *Phys. Rev. Lett.* **74**, 3939 (1995).
- [17] R. G. Thomas, *Prog. Theor. Phys.* **12**, 253 (1954).
- [18] A. Insolia, P. Curutchet, R. J. Liotta, and D. S. Delion, *Phys. Rev. C* **44**, 545 (1991); D. S. Delion, A. Insolia, and R. J. Liotta, *ibid.* **46**, 1346 (1992); **46**, 884 (1992); **49**, 3024 (1994).
- [19] C. Pomar, J. Blomqvist, R. J. Liotta, and A. Insolia, *Nucl. Phys.* **A515**, 381 (1990).
- [20] I. Tonozuka and A. Arima, *Nucl. Phys.* **A323**, 45 (1979).
- [21] P. Ring and P. Schuck, *The Nuclear Many-Body Problem* (Springer-Verlag, New York, 1980).
- [22] M. W. Herzog *et al.*, *Nucl. Phys.* **A448**, 441 (1986).
- [23] M. Guttormsen, *Phys. Lett.* **105B**, 99 (1981).
- [24] G. D. Dracoulis, A. E. Stuchbery, A. P. Byrne, A. R. Poletti, J. Gerl, and R. A. Bark, *J. Phys. G* **12**, L97 (1986).
- [25] K. Heyde and R. A. Meyer, *Phys. Rev. C* **37**, 2170 (1991).
- [26] R. Bengtsson, J. Dudek, W. Nazarewicz, and P. Olanders, *Phys. Scrip.* **39** 196 (1989); S. Cwiok, J. Dudek, W. Nazarewicz, J. Skalski, and T. Werner, *Comput. Phys. Commun.* **46**, 379 (1987).
- [27] J. Wauters *et al.*, *Phys. Rev. C* **47**, 1447 (1993).
- [28] P. Dendooven *et al.*, *Phys. Lett. B* **226**, 27 (1989).